ASTM INTERNATIONAL
Selected Technical Papers

Zirconium in the Nuclear Industry

17th International Symposium

STP 1543

Editors
Robert J. Comstock
Pierre Barbéris

SELECTED TECHNICAL PAPERS
STP1543

Editors: Robert Comstock, Pierre Barbéris

Zirconium in the Nuclear Industry: 17th International Symposium

ASTM Stock #STP1543

ASTM International, 100 Barr Harbor Drive, PO Box C700, West Conshohocken, PA 19438-2959.
Printed in the U.S.A.

Library of Congress Cataloging-in-Publication Data

ISBN: 978-0-8031-7529-7
ISSN: 1050-7558

Peer Review Policy
Each paper published in this volume was evaluated by two peer reviewers and at least one editor. The authors addressed all of the reviewers' comments to the satisfaction of both the technical editor(s) and the ASTM International Committee on Publications.

The quality of the papers in this publication reflects not only the obvious efforts of the authors and the technical editor(s), but also the work of the peer reviewers. In keeping with long-standing publication practices, ASTM International maintains the anonymity of the peer reviewers. The ASTM International Committee on Publications acknowledges with appreciation their dedication and contribution of time and effort on behalf of ASTM International.

Citation of Papers
When citing papers from this publication, the appropriate citation includes the paper authors, "paper title", STP title, STP number, book editor(s), page range, Paper doi, ASTM International, West Conshohocken, PA, year listed in the footnote of the paper. A citation is provided on page one of each paper.

Printed in Bay Shore, NY
January, 2015

Foreword

This Compilation of *Selected Technical Papers*, STP1543, *Zirconium in the Nuclear Industry: 17th International Symposium*, contains peer-reviewed papers that were presented at a symposium held February 3–7, 2013 in Hyderabad, India. The symposium was sponsored by ASTM International Committee B10 on Reactive and Refractory Metals and Alloys and Subcommittee B10.02 on Zirconium and Hafnium.

The Symposium Co-Chairmen were Pierre Barbéris, Areva/Cezus Research Centre, Ugine, France and Srikumar Banerjee, Atomic Energy Commission, Anushakti Bhavan, Mumbai, India.

The STP Editors are Robert J. Comstock, Westinghouse Electric Company, Pittsburgh, PA, USA and Pierre Barbéris.

Contents

Fabrication

Corrosion and Hydrogen Pickup

In Reactor Performance

Irradiation and Hydrogen Effects

High Temperature Transient Behavior

Degradation and Failure Mechanisms

Overview

This STP contains the papers presented at the *17th International Symposium on Zirconium in the Nuclear Industry* held in Hyderabad, Andhra Pradesh, India from February 3–7, 2013. The first symposium was held in Philadelphia in 1968 with subsequent symposia held every two to three years. The proceedings of each symposium in the series have been documented with an STP.

During this symposium, the William J. Kroll Zirconium Medal was presented to John Kearns (2011 winner) and Srikumar Banerjee (2012 winner) for their unique and lasting contributions to the technology of zirconium alloys. Both provided historical perspectives of their research during the symposium and contributed papers that are included in the STP.

The symposium was truly international; with approximately 130 participants from 17 countries attending and representation from North and South America, Europe, and Asia. The 17th Symposium included 42 platform presentations along with a session with 31 posters. This STP contains 38 peer reviewed papers along with the papers from the two Kroll winners. In addition, the discussion of each platform presentation provided an opportunity for further insight and understanding of the paper. As in past symposia, the questions along with written responses by the authors are included at the end of each paper.

The symposium is an opportunity to capture a snapshot of the current research areas that are relevant to the nuclear industry. This symposium was no exception. While the papers are grouped into seven categories (*Basic Metallurgy and Alloying Effects, Fabrication, Corrosion and Hydrogen Pickup, In Reactor Performance, Irradiation and Hydrogen Effects, High Temperature Transient Behavior,* and *Degradation and Failure Mechanisms*), there is often overlap between the topics as you will see when you browse through the STP or delve into papers more deeply.

An important component of the symposium is the in-reactor performance of zirconium alloys with several papers presenting recent results from materials irradiated to high burnups and fluence.

- Alloy E635 was irradiated to 72 MWd/kgU in VVER-1000 reactors with performance data presented from both fuel cladding and structural components. The behavior of the material was correlated to both temperature and neutron fluence.
- The evolution of the microstructure of M5™ fuel rod cladding irradiated in a PWR up to 7 cycles with fast fluence up to 17.1×10^{25} n/m^2 was described. In a separate paper, results from M5™ with 1000 ppm Fe (designated M5-Fe)

included both oxide thickness measurements at burnups of about 65 MWd/tU and free growth at fluences to 20×10^{25} n/m^2 (E > 1Mev).

- ZIRLO® structural components were characterized for both corrosion and dimensional changes following irradiation in PWRs with a maximum fluence of 13.6×10^{25} n/m^2 (E > 1Mev).
- Optimized ZIRLO™ fuel cladding was irradiated beyond the license limit of 62 GWd/MTU to 70 GWd/MTU. Characterization of the cladding included corrosion, dimensional changes, and mechanical properties.
- A detailed study was presented on the influence of temperature and microstructure on the irradiation creep behavior of Zr-2.5Nb pressure tubes.

A dominant theme in this STP is the role of hydrogen on the performance of zirconium alloy components. Issues discussed in this volume where performance was dominated by hydrogen included the following:

- Failure of BWR fuel rods was attributed to the localization of hydrides following accelerated corrosion and subsequent cracking of the hydride lenses. Despite an extensive investigation, the cause of the accelerated corrosion was not definitively identified.
- The growth of beta-quenched Zircaloy-2 BWR channels was driven late in life by accelerated hydrogen pickup that coincided with the dissolution of second phase particles.
- As reorientation of hydrides plays an important role during dry storage, in-situ measurements were performed to gain new insights into the reorientation of hydrides in Zircaloy-4.
- Delayed hydride cracking (DHC) growth rate of in-service Zr-2.5Nb CANDU pressure tubes was controlled by thermal and irradiation effects on the microstructure (e.g, decomposition and reconstitution of the beta phase controlling hydrogen diffusion to the crack tip).

In addition to papers that highlight the impact of hydrogen, several papers focused on understanding the mechanisms of hydrogen ingress into the metal or understanding the interaction of hydrogen with point defects and dislocation loops in the matrix. The latter has potential implications related to hydrogen assisted irradiation growth.

The US Nuclear Regulatory Commission proposal of a rule to amend the current requirements governing emergency core cooling system for light nuclear power reactors has prompted renewed activity in cladding ductility following a high temperature transient. Papers addressed different aspects of the high temperature oxidation behavior of cladding, including secondary hydriding following rod burst, the detrimental role of nitrogen on oxidation kinetics, and the impact of a pre-oxide or steam pressure on oxidation and subsequent cladding ductility. One paper demonstrated

the improved oxidation performance of E110G relative to E110. Unfortunately, the reason for the improvement remains an area for continued research.

In response to the Fukushima Daiichi nuclear accident in March, 2011, significant attention has been given to improving the accident tolerance of zirconium alloy fuel cladding. Researchers presented one approach through the application of coating technology to improve the high temperature oxidation resistance of the cladding. While significant development work remains, this is an area that will likely receive continued attention to identify viable options.

The zirconium community continues to push the limits of state-of-the-art analytical techniques to characterize the microstructure of both non-irradiated and irradiated zirconium alloys. Techniques such as synchrotron radiation (e.g., μ x-ray absorption near edge spectroscopy, diffraction, and stress measurement), electron back-scattered diffraction, atom probe tomography, secondary ion mass spectroscopy, and electron energy loss spectroscopy have become routine analytical tools in multiple laboratories around the world. Cold neutron prompt gamma activation analysis was successfully used in one study to non-destructively measure hydrogen content in corrosion coupons. Complementing the analytical characterization techniques are modelling efforts designed to facilitate mechanistic understanding of performance phenomena.

Following the symposium, a committee of technical experts covering a breadth of experience in the zirconium nuclear industry selected the best paper based upon technical excellence, relevance to the nuclear industry, and 'groundbreaking' research. The winner of the John H. Schemel Best Paper Award was the paper entitled "Effect of Hydrogen on Dimensional Changes of Zirconium and the Influence of Alloying Elements: First-Principles and Classical Simulations of Point Defects, Dislocation Loops, and Hydrides" by M. Christensen, W. Wolf, C. Freeman, E. Wimmer, R. B. Adamson, L. Hallstadius, P. Cantonwine, and E. V. Mader. Congratulations to the winners.

Robert J. Comstock
Pierre Barbéris

ASTM INTERNATIONAL
Helping our world work better

ISBN: 978-0-8031-7529-7
Stock #: STP1543

www.astm.org

STP 1543, 2015 / available online at www.astm.org / doi: 10.1520/STP154320120165

Zoltán Hózer,[1] Erzsébet Perez-Feró,[1] Tamás Novotny,[1]
Imre Nagy,[1] Márta Horváth,[1] Anna Pintér-Csordás,[1]
András Vimi,[1] Mihály Kunstár,[1] and Tamás Kemény[2]

Experimental Comparison of the Behavior of E110 and E110G Claddings at High Temperature

Reference

Hózer, Zoltán, Perez-Feró, Erzsébet, Novotny, Tamás, Nagy, Imre, Horváth, Márta, Pintér-Csordás, Anna, Vimi, András, Kunstár, Mihály, and Kemény, Tamás, "Experimental Comparison of the Behavior of E110 and E110G Claddings at High Temperature," *Zirconium in the Nuclear Industry: 17th International Symposium*, STP 1543, Robert Comstock and Pierre Barberis, Eds., pp. 932–951, doi:10.1520/STP154320120165, ASTM International, West Conshohocken, PA 2015.[3]

ABSTRACT

A new experimental program was carried out in order to compare the behavior of E110 and E110G type alloys at high temperature. The program included differential scanning calorimetry studies on the phase transition process, ballooning and burst tests, oxidation in steam and hydrogen rich steam atmospheres, ring compression tests of oxidized samples and posttest examination with optical and scanning electron microscopes.The two alloys showed very similar behavior in the non-oxidized state. The phase transitions took place practically in the same range of temperature and the cladding burst due to ballooning also happened under similar conditions. The oxidation caused significant differences. The breakaway oxidation typical for E110 could not be observed with E110G samples. The E110G had much better load bearing capabilities in oxidized state and did not pick up as much hydrogen as the other alloy did.

Keywords

Zirconium oxidation, cladding embrittlement, ballooning and burst

Manuscript received November 19, 2012; accepted for publication November 3, 2013; published online June 17, 2014.

[1]Centre for Energy Research, Hungarian Academy of Sciences, Budapest, Hungary H-1525.
[2]Wigner Research Centre for Physics, Hungarian Academy of Sciences, Budapest, Hungary H-1525.

[3]ASTM 17th International Symposium on *Zirconium in the Nuclear Industry* on February 3–7, 2013 in Hyderabad, India.

Introduction

The E110 type cladding has been used in VVER reactors for many decades in different countries [1–3]. The E110 cladding has outstanding corrosion resistance during normal operation in the reactors. After four cycles and up to 65 MWd/kgU burnup, the thickness of an oxide scale on the external surface of the cladding does not exceed 10 μm and the hydrogen content remains below 120 ppm [4–6]. The behavior of E110 at high temperature (especially in the range of 900°C–1000°C) is characterized by breakaway oxidation, high hydrogen uptake, and embrittlement at low degree of oxidation compared to other zirconium alloys, as, e.g., Zircaloy-4 [7–11].

The E110 cladding is traditionally produced on electrolytic basis. The Russian fuel supplier intends to introduce the production of cladding tubes from sponge material [12]. The new alloy named E110G is characterized by the same composition as E110, but some preliminary tests indicated significant differences in the behavior of the two alloys at high temperatures [7].

In order to cover a wide range of parameters for loss-of-coolant-accident (LOCA) conditions, a systematic experimental program has been carried out in Hungary. The main objectives of the tests were to compare the behavior of the two alloys at high temperatures and to produce E110G specific data for the development of numerical models that can be built into transient fuel behavior codes and used in safety analyses. The program included the following elements:

- determination of the composition of the alloys,
- phase transition studies,
- ballooning and burst of tube samples with inner pressurization,
- oxidation in steam atmosphere,
- oxidation in hydrogen rich steam atmosphere,
- investigation of breakaway effect,
- mechanical testing of oxidized cladding samples,
- determination of the hydrogen content of oxidized samples,
- post-test examination of samples by optical and scanning electron microscopy.

Experimental Details

COMPOSITION

The composition of the investigated E110 and E110G cladding tubes was determined with an AEI MS702/R type spark source mass spectrometer (SSMS) with Mattauch–Herzog geometry. 10 mm long and 1 mm wide electrodes were produced from the cladding tubes. The samples were degreased with acetone and alcohol before testing. High voltage (20 kV) power with 100 pulse/s frequency and 100 μs length was applied to ionize the samples. The spectra were recorded on traditional photo plates (Ilford Q2) and evaluated using a Zeiss MD-100 microdensitometer. There were no available zirconium standards to determine the correct Relative Sensitivity Coefficient (RSC) values for the analyzed elements. RSC values were taken

from earlier studies and ^{93}Nb (1 % content) and ^{96}Zr (2.8 % abundance) isotopes were used as internal standards.

PHASE TRANSITION

The phase transition process was investigated by Differential Scanning Calorimetry (DSC) method. Small pieces of E110G and E110 tubes were placed in a sample holder with Al_2O_3 powder. For calibration purposes, a few mg of Ag was added to the reference sample holder. The measurements were carried out at four different heating rates: 2.5, 5, 10, and 20°C/min. Control measurement was performed with pure Zr. The DSC measurements were carried out at the Material Physics Dept., Eötvös University, Budapest.

OXIDATION

The oxidation of E110G cladding was investigated in a high temperature furnace. A steam generator with controllable power supply provided steam for the experiments. The tube type furnace was placed in horizontal position and it had three heating sections with microprocessor control. The inlet junction of the furnace was connected to the steam generator. The remaining steam fraction of the outlet gas was condensed in the condenser unit. A quartz tube with 19 mm diameter was used inside of the furnace. Additional electrical heaters were installed in the inlet and outlet connecting tubes to prevent condensation in the facility (Fig. 1).

In order to investigate breakaway phenomena, the experimental facility was connected to a thermoconductometric detector (TCD) of a gas-chromatograph. The signal of the TCD was proportional to the concentration of the hydrogen in the outlet gas and thus it indicated the intensity of oxidation process.

FIG. 1 Scheme of the high temperature furnace used for cladding oxidation.

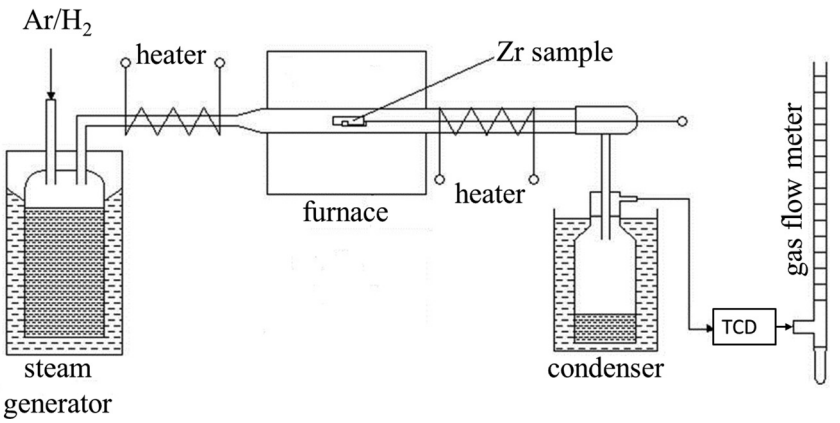

The tests were carried out with 8 mm long fuel cladding samples cut from the original cladding tubes. The external diameters of the E110 and E110G tubes were 9.14 and 9.10 mm, respectively. The cladding thickness was 0.65 mm for both materials. In most of the experiments, two samples were placed in the furnace: one E11G and one E110 sample, in order to have the same oxidizing conditions and to allow the direct comparison of the two alloys. The vertically positioned samples were standing one after another in the horizontal sample holder, which had contact with the bottom rim of the samples. The samples did not touch each other and both samples were in the uniform temperature section of the furnace. Acetone was applied to degrease the samples before testing. The masses of samples before and after oxidation were carefully measured. The extent of cladding oxidation was expressed as measured Equivalent Cladding Reacted (ECR) and it was calculated on the basis of mass gain: $ECR = \frac{A_{Zr} \cdot \Delta m}{M_{O_2} \cdot m_i} \cdot 100$, where A_{Zr} = molar mass of zirconium, M_{O_2} = molar mass of oxygen, m_i = mass of sample before oxidation, and Δm = mass gain during oxidation.

At the beginning of the tests, the furnace was heated up to the target temperature without the samples. After stabilization of thermal conditions, the samples were moved from the unheated zone of the quartz tube into the center of furnace.

Isothermal tests in steam atmosphere were performed between 600°C–1200°C. The steam was mixed with 12 v/v% high purity argon carrier gas. This argon content does not influence the oxidation process, but it is needed to stabilize gas flow in the outlet section of the furnace. The steam supply was constant during the tests and the flow rate was high enough to prevent steam starvation inside of the furnace. The typical steam flow was 4–4.5 mg/cm^{2}s, while the starvation threshold even at 1200°C remained below 3.5 mg/cm^{2}s for the given sample geometry.

The breakaway oxidation test series covered the temperature range of 800°C–1200°C and only single samples were used in order to avoid any potential interference between the signals originated from the two different alloys and to characterize the E110G and E110 samples separately. The typical oxidation time was 2700 s.

Additional tests series were conducted to investigate the effect of high hydrogen content in the steam atmosphere. These tests were carried out in the temperature range of 900°C–1100°C with 65 v/v% hydrogen content in the steam. This hydrogen content was selected in order to have comparable conditions to the earlier experiment with E110 cladding [11].

BALLOONING AND BURST

The plastic deformation of cladding tubes at high temperature was investigated in ballooning tests with inner pressurization of cladding tubes in a vertical tube furnace. The experiments were carried out under isothermal conditions. The samples were placed in the center of the furnace where the axial temperature profile was uniform.

FIG. 2 Drawing of the sample used in ballooning tests.

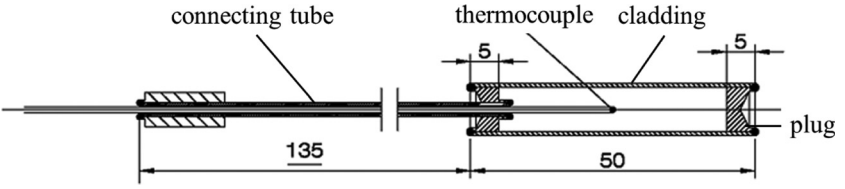

The samples were produced from original cladding tubes. Both ends of the 50 mm long tubes were closed by welded Zr plugs, but one of them had an internal hole for the connecting tube (Fig. 2). The pressurization of the samples was performed through this small diameter Zr connecting tube. The pressurization of the samples was driven by a control unit using capillary tubes, needle valves, and a stepper motor. The linear pressurization was continued until the burst of the sample (Fig. 3). The temperature and pressure histories were recorded during the tests.

The basic series of ballooning tests was performed with non-oxidized samples in argon atmosphere. In order to investigate the effect of oxidation, some samples were pre-oxidized before the ballooning test in the oxidation facility (Fig. 1) in steam atmosphere at 900°C. The isothermal tests were conducted between 700°C–1200°C. The pressurization rates covered three orders of magnitude from 0.007 bars/s to 7 bars/s.

FIG. 3 Pressure and temperature histories in ballooning test at 800°C with pressurization rate 0.007 bars/s.

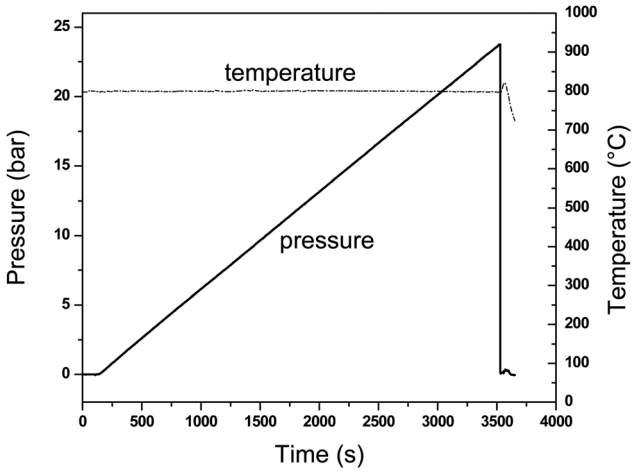

After the tests, post-test examination of the samples was carried out and the average and maximum values of deformation were determined.

MECHANICAL TESTING

Mechanical testing of oxidized E110G and E110 ring samples was carried out with an INSTRON 1195 type tensile testing machine. A special heater module can be mounted to the machine for testing at high temperature.

Ring compression tests were performed at room temperature and at 135°C. In case of high temperature testing, the temperature in the machine was stabilized before starting the mechanical loading. The speed of the cross head was 0.5 mm/min. The load-displacement curves were recorded during the ring compression tests.

POST-TEST EXAMINATION

Metallography examination of oxidized samples was carried out with a Reichert type optical microscope. A Philips SEM 505 type scanning electron microscope and a JEOL Superprobe 733 type microprobe were also used to investigate the cladding microstructure.

The hydrogen content of the oxidized Zr samples was determined by hot extraction method at 1150°C using a CHROMPACK 438 A type gas cromatograph.

Results and Discussion

COMPOSITION

The main alloying element in both E110 and E110G is Nb with 1 %. The SSMS measurements indicated that impurities are higher in E110G than in E110, except Ni and Hf (Table 1). Significant differences were found for hafnium and iron. The hafnium content was intentionally decreased in the new alloy from 100 ppm to 10 ppm in order to reduce neutron absorption by the cladding. The iron content was increased in the new cladding from 50 ppm to 500 ppm value. According to

TABLE 1 Impurities present in E110 and E110G alloys.

Element	E110	E110G
Mg	0.5 ppm	1.5 ppm
Al	0.5 ppm	10 ppm
Si	1 ppm	35 ppm
Cr	10 ppm	30 ppm
Mn	0.1 ppm	5 ppm
Fe	45 ppm	500 ppm
Ni	15 ppm	15 ppm
Cu	0.5 ppm	5 ppm
Hf	100 ppm	10 ppm

Nikulin et al. [12], the sum of the following impurities (C, Si, Ni, P, Cl, N, F, and Al) was about 140 ppm in E110 and about 70 ppm for E110G. Further analysis of impurities present in E110 and E110G is required to more clearly establish the difference between the materials.

PHASE TRANSITION

The DSC measurements indicated that phase transition took place for E110G cladding between 800 and 930°C. The higher heating rate resulted in higher temperature for both onset and end of phase transition (**Fig. 4**). The measured data showed ≈100°C difference between the onset and end of phase transition, which is in good agreement with the results of previous studies [13].

OXIDATION

The comparison of mass gains of E110G and E110 during oxidation in steam indicated two types of oxidation kinetics (**Fig. 5**).

- At 600, 700, and 800°C the E110G reached a higher degree of oxidation in all measured points. However, this difference is rather small, e.g., the oxidation at 800°C for 2 h resulted in 3.7 % ECR for E110G and 2.9 % ECR for E110. So the relative difference for this point is only 27 %. At 1100 and 1200°C, the E110G oxidized faster, too. Oxidation at 1100°C for 1700 s created 20.7 % ECR for E110G and 16.6 % for E110. The relative increase in this case was 25 %. The comparison with weight gain calculated using the Cathcart–Pawel correlation indicates that the oxidation kinetics was slower at 600, 700, and 800°C for both E110 and E110G alloys. It is not surprising, since the correlation is valid above 1000°C. At 1100 and 1200°C, the correlation is in very

FIG. 4 Onset and end temperatures of E110 and E110G phase transition (DSC data).

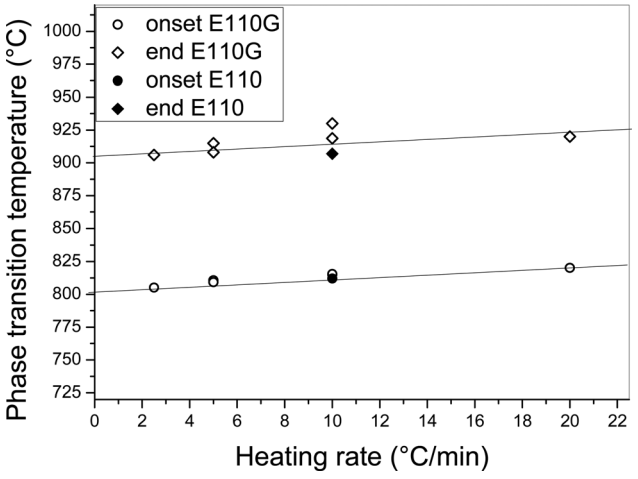

FIG. 5 Results of oxidation of E110G and E110 samples in steam at 800 and 1000°C.

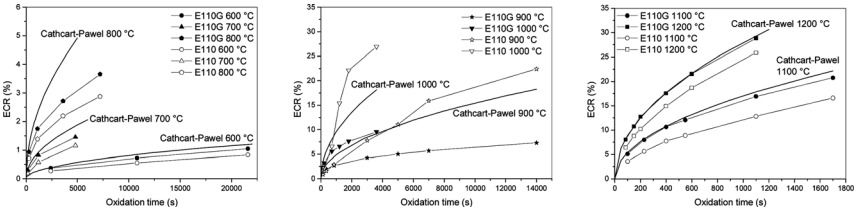

good agreement with the E110G oxidation data and slightly overestimates the E110 oxidation kinetics.

- At 900 and 1000°C, the oxidation of E110 was much more intense than that of E110G. At 900°C, the oxidation of E110G is much slower than that of E110 and also much less than predicted by the Cathcart–Pawel correlation (**Fig. 5**).
- The oxidation at 1000°C for 1 h lead to 9.5 % ECR for E110G, while it produced 26.9 % ECR for E110. The relative difference in this case was 283 %. The Cathcart–Pawel correlation gives 18.1 % ECR for this oxidation time at 1000°C. The start of breakaway oxidation can be observed on the E110 curve after ≈800 s, where the oxidation kinetics significantly accelerates compared to E110G data and to the Cathcart–Pawel correlation.

The most significant difference between the oxidation behavior of E110 and E110G alloys was found at 900 and 1000°C, where the E110 cladding is characterized by intense breakaway oxidation. The oxidation process could be described by parabolic functions of time with the exception of E110 oxidation at 900 and 1000°C.

The oxidation in hydrogen rich steam showed that the hydrogen content in the atmosphere does not change the oxidation kinetics. The mass gains of samples oxidized in steam with and without hydrogen were very close to each other for both E110 and E110G. The difference between the ECRs of two alloys was practically the same for the cases with and without hydrogen in the atmosphere (**Fig. 6**).

BREAKAWAY EFFECT

The visual observation of ring samples after oxidation in pure steam and in hydrogen rich steam indicated significant differences. The oxide scale on the E110G samples was always compact, while on the surface of the E110 samples in many cases—especially after long oxidation at 900 and 1000°C—spalling oxide scales could be observed (**Fig. 7**).

The breakaway effect was detected in the tests with on-line H release measurements, too. The first peak of the TCD signal (**Fig. 8**) indicated the intense start of oxidation process. After the peak, the signal for E110G started to monotonously decrease since the developed compact oxide layer played a protective role and slowed down the oxidation process. In case of E110 at 1000°C the TCD signal did

FIG. 6 Results of oxidation of E110G and E110 samples in hydrogen rich steam at 900°C.

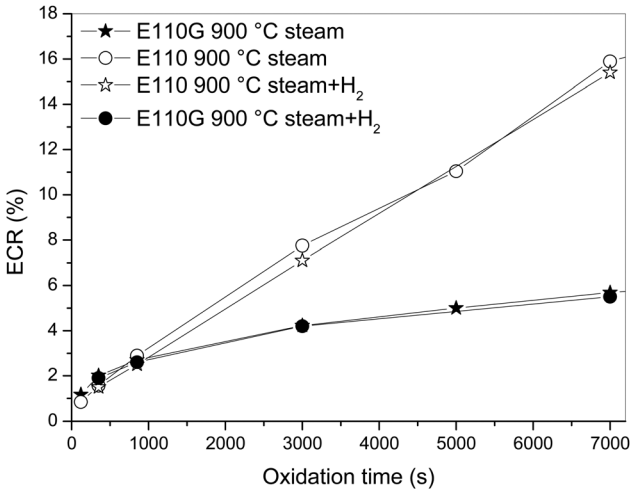

not decrease monotonously, but it was characterized by several local peaks and local minima. The acceleration of hydrogen production after each local minimum showed that the oxide layer spalled and the direct contact between the metal surface and the atmosphere resulted in intense oxidation. A development of the compact oxide layer continued until the next local minimum. For E110G, breakaway oxidation could not be observed in the investigated range of temperatures and oxidation times, even in case of 7200 s oxidation at 1000°C.

The reason for the different breakaway behavior of Zr claddings was analyzed by several authors in the past. Chung [14] pointed out that some impurities (e.g., fluorine) are deleterious, and can lead to increased susceptibility to nodular oxidation. He emphasized that Zr metal produced by electrolysis contains F, while Kroll

FIG. 7 View of E110G (left) and E110 (right) cladding samples after 5000 s oxidation at 900°C in steam.

FIG. 8 Comparison of hydrogen release in case of E110 and E110G cladding at temperature 1000°C.

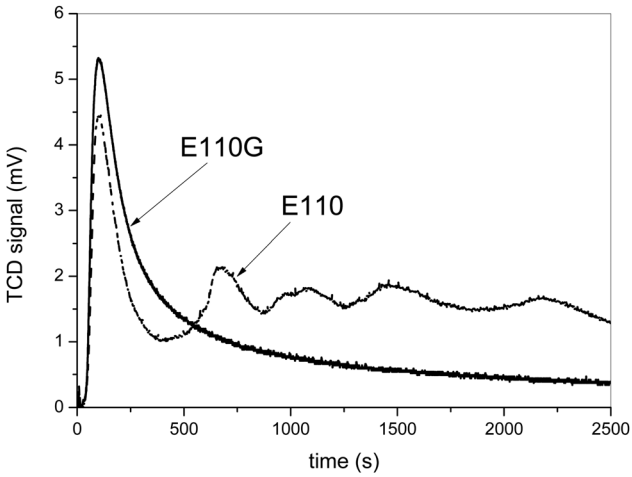

fabrication process prevents F pickup. Yan et al. [9] carried out experiments with polished E110 samples. Smooth, black oxide was formed on the polished surface during steam oxidation, while cracked, delaminated oxide layer could be observed on the as-received E110 surface. Yegorova et al. [15] examined several advanced types of El10 claddings manufactured on the basis of sponge Zr to evaluate the sensitivity of the oxidation phenomena to the bulk chemistry of the cladding material. They concluded that the best way for the improvement of the corrosion resistance of E110 cladding could be the fabrication of cladding material from sponge Zr and the application of polishing to the internal and external surfaces of the tubes. The E110 and E110G cladding tubes used in the present study were produced by the same technology in the fuel factory. The only difference was that sponge ingot was used for E110G instead of traditional electrolytic ingot. It means that the surface of the two tested materials were the same (they were produced in the same factory by the same production line), while the content of some impurities were different, and it can lead to the differences observed at high temperature oxidation.

BALLOONING AND BURST

The ballooning tests showed that cladding burst pressure decreased with the increase of temperature. The 800°C sample pressurized with 2.6 bars/s rate burst at 87.8 bars, while the sample at 1200°C with the same pressurization rate failed at 15.4 bars.

The pressurization rate had a very important effect on burst pressure. For example, the cladding tube tested at 800°C with 0.007 bars/s load lost its integrity at 23.7 bars, while the pressurization rate of 7.1 bars/s resulted in burst at 115 bars. Similar tendency could be observed for other temperatures, too (Fig. 9).

FIG. 9 Burst pressure of E110G tubes as function of pressurization rate.

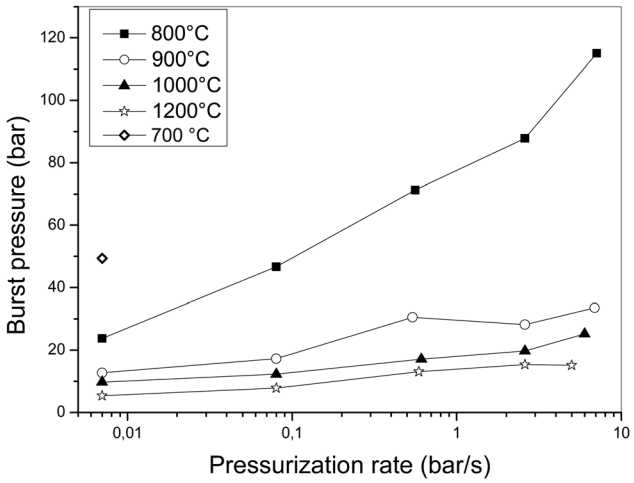

The deformation of the tube due to ballooning reached about 100 % at 700 and 800°C. At higher temperatures the deformations were smaller, between 1000 and 1200°C the typical values were 10 %–40 % (**Fig. 10**). Furthermore, the faster pressurization lead to larger deformations.

The comparison of new E110G data with previously measured E110 data [13] indicated that failure of E110G cladding took place at slightly higher pressure than E110. **Figure 11** shows some measurement points with 0.08 bars/s pressurization rate. The burst pressure for the E110G is higher for all samples. The figure shows consistent small differences between the two materials. Similar behavior was observed at other pressurization rates for most of the measured points.

Earlier tests indicated that the initial oxide layer can increase the mechanical strength of the E110 cladding [11,13] up to some degree of oxidation. After reaching a maximum value, the further oxidation leads to strong embrittlement and failure at lower loads. This effect was observed in the current test series with E110G cladding, too. The maximum values for both E110 and E110G corresponded to

FIG. 10 Ballooned E110G samples (left: 700°C and 0007 bars/s, center: 900°C and 0,6 bars/s, right: 1200°C and 6 bars/s).

FIG. 11 Comparison of the burst pressures of E110 and E110G claddings at 0.08 bars/s pressurization rate.

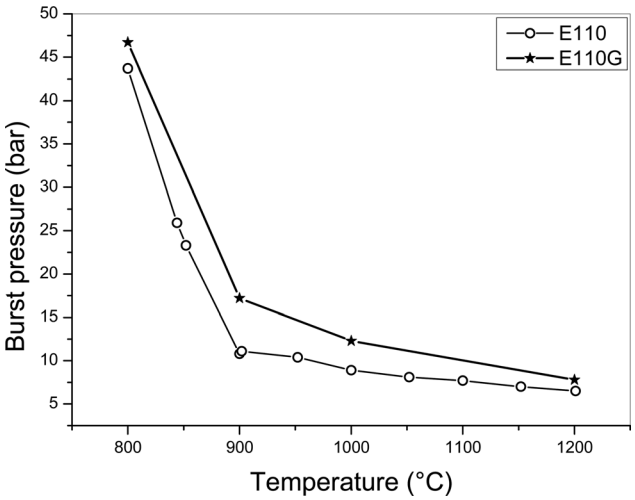

20 μm oxide scale (Fig. 12). It must be mentioned that the pre-oxidation was performed at 900°C, where the E110 alloy shows a short time to breakaway. The maximum burst pressure in Fig. 12 with 20 μm oxide scale corresponds to 400 s

FIG. 12 Burst pressure of oxidized E110G and E110 sample tested at 800°C with 0.025 bars/s pressurization rate.

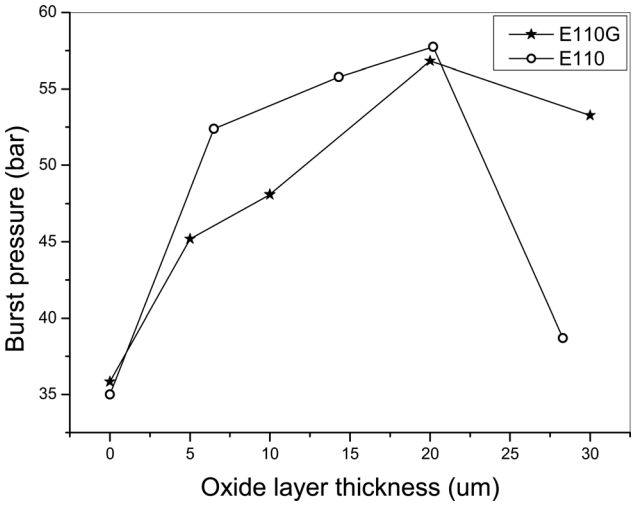

oxidation time for E110 cladding and 5150 s for E110G. As such, in accident conditions, significant differences exists in the burst behavior of the oxidized claddings.

MECHANICAL TESTING OF OXIDIZED SAMPLES

The ring compression tests produced similar load-displacement curves for E110 and E110G samples with low degree of oxidation. The increase of ECR, however, proved that the new E110G cladding had much better load bearing capability compared to E110. The most significant differences were found for the samples oxidized at 900 and 1000°C. This is the same interval, where the oxidation of E110 was much more intense than that of E110G. Figure 13 shows the load-displacement curves of two samples that were oxidized parallel at 1000°C for 1 h. The E110G could be loaded in the tensile test machine up to 550 N and a curve showed ductile character. The E110 sample failed at 120 N and the curve showed the typical form of brittle material. Similar effect was seen for many other pairs of samples were oxidized not only in steam but in hydrogen rich steam atmosphere as well.

On the basis of ring compression tests, the ductile-to-brittle transition of oxidized samples was determined. The analyses of the load-displacement curves allowed us to distinguish between ductile and brittle samples. In case of ductile samples the elastic deformation is followed by a plastic plateau, while in case of brittle material, the breakdown of the curve indicates the brittle failure of the ring after the elastic deformation. In most cases, the peak of the curves of brittle materials does not reach as high values as the ductile ones do. Furthermore, the integral of

FIG. 13 Load-displacement curves of E110G and E110 ring samples oxidized at 1000°C for 3600 s.

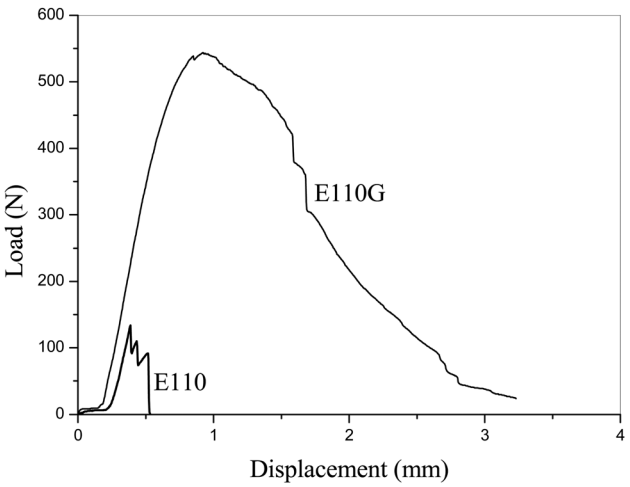

the curves of up to the first breakdown (indicating the accumulated energy to failure) has much lower values compared to ductile samples with similar geometry.

In Fig. 14, each oxidized sample is marked as ductile or brittle. The transition line, representing the ductile-to-brittle transition limit, was drawn to separate the points in a conservative way: all the brittle points and a few ductile points are above the line, and the remaining ductile points are below the line. This approach guarantees that the cladding has some ductility under the oxidation conditions below the line. These lines in Fig. 14 can be described by an Arrhenius type equation: the time of oxidation to reach brittle state is proportional to the exponent of the reciprocal of absolute temperature. The application of such functions facilitates the integration of the degree of embrittlement during transient conditions and can be used in safety analyses [8]. The difference in time between the two materials is only apparent at 900 and 1000°C, where E110 shows high oxidation accumulation (breakaway effect).

Comparing the two transition lines it can be seen (Fig. 14) that the E110G transition is shifted to higher temperatures and longer oxidation times. At a given oxidation time this shift means 130°C, or at a fixed temperature four times longer oxidation. Testing of samples oxidized at 135°C proved that transition to brittle failure of oxidized Zr rings took place at higher degree of oxidation than at room temperature.

POST-TEST EXAMINATIONS

The post-test examinations pointed out some microstructural differences between the two alloys in oxidized state. Figure 15 shows that the oxide scale on E110 alloy had a layered structure that is typical for breakaway oxidation. The micrograph shown is typical only when there is breakaway oxidation for E110. On the surface of the E110G sample oxidized together with the E110 ring, a compact oxide layer was formed. The average thickness of the E110G sample was 24 μm, while the E110 cladding had several 10–20 μm layers of oxide with the total thickness of 89 μm.

FIG. 14 Ductile-to-brittle transition of oxidized E110 and E110G samples based on ring compression tests at room temperature.

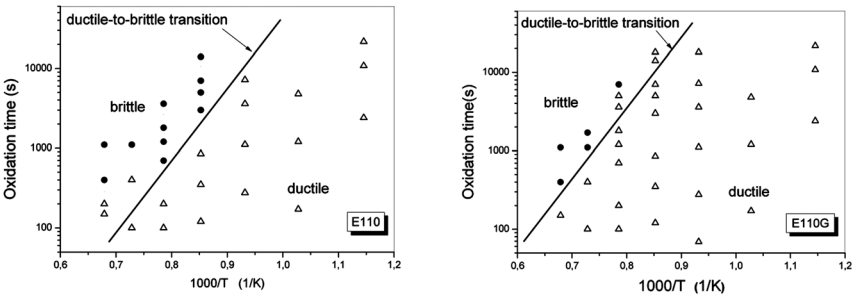

FIG. 15 Metallography pictures of E110 (left) and E110G (right) after oxidation at 1000°C for 3600 s.

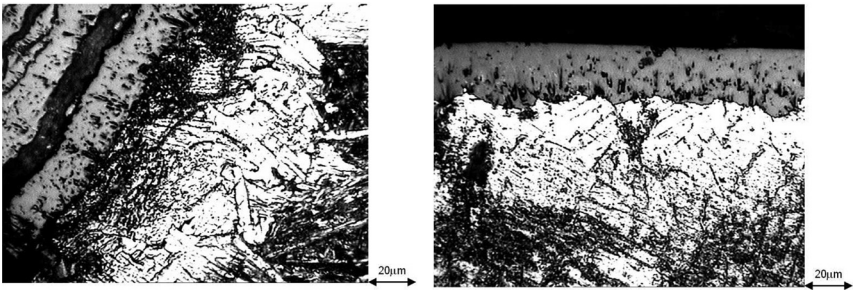

The secondary electron images (SEI) taken during SEM analyses indicated that the E110 sample oxidized at 1000°C for 3600 s failed due to brittle fracture in the ring compression test, for the microstructure was characterized by large plates (**Fig. 16**). The fracture surface of the counterpart E110G sample showed small scale honeycomb structure that is typical for ductile deformation.

The oxide scale thicknesses were determined during metallography examination. The two alloys had similar thicknesses at the same ECRs (**Fig. 17**), but it must be emphasized that the same ECRs were reached in different oxidation times. **Figure 17** includes data from different temperatures between 900 and 1200°C.

The hydrogen content in selected samples showed also significant differences between the two alloys. The H uptake of the examined E110G samples was below the detection limit (100 ppm), while some oxidized E110 samples contained several thousand ppm hydrogen. For example, in case the samples oxidized at 1000°C for 3600 s (**Figs. 13**, **15**, and **16**) the hydrogen content in E110G was less than 100 ppm,

FIG. 16 Secondary electron images of the fracture surfaces of E110 (left) E110G (right) samples after oxidation at 1000°C for 3600 s and ring compression testing.

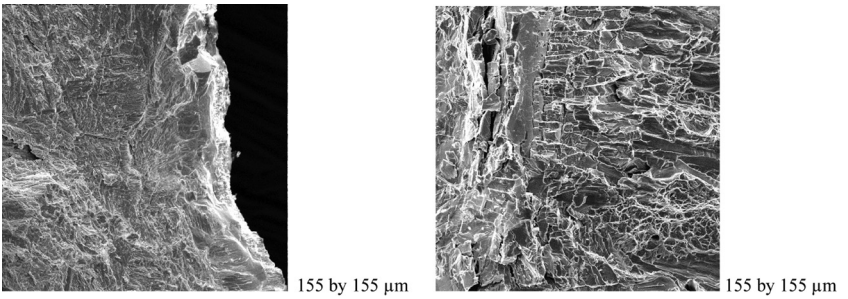

FIG. 17 Oxide layer thickness as function of ECR for E110 and E110G alloys oxidized in steam.

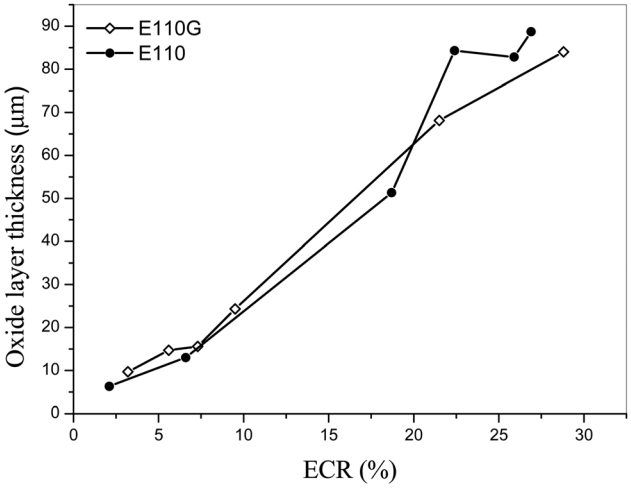

but the E110 ring had 3990 ppm hydrogen. The data points in Fig. 17 are characterized with hydrogen content below 100 ppm for all the points, except E110 samples above 15 % ECR, which contained 3530–5720 ppm hydrogen.

Conclusions

The high temperature behavior of E110 and E110G type alloys was compared through a series of experiments. The experimental program covered most of the cladding related phenomena that can take place during a LOCA event in a nuclear reactor.

The experimental program included differential scanning calorimetry and thermomechanical studies on the phase transition process. The plastic deformation and the burst of cladding was investigated in isothermal ballooning tests in the temperature range of 600°C–1200°C with linear pressurization rates of 0.007–7 bars/s. Oxidation of samples was carried out in steam atmosphere between 600°C–1200°C and in hydrogen rich steam atmosphere between 900°C–1100°C. Special studies were devoted to the investigation of breakaway oxidation in steam atmosphere with online hydrogen detection. The mechanical load bearing capability of the oxidized samples was investigated through ring compression tests at room temperature and at 135°C. Optical and scanning electron microscopy examinations were performed and the hydrogen content was determined for selected oxidized samples.

The results of phase transition studies and ballooning tests showed that, without oxidation, the behavior of the two alloys was well comparable in the

investigated range of parameters. The oxidation, however, resulted in significant differences, especially at 900 and 1000°C. The E110 samples had typically layered oxide scale due to breakaway phenomena. In case of E110G, the breakaway process did not take place and compact oxide layers could be observed on all samples. According to the mechanical tests, the ductile-to-brittle transition for the oxidized E110G alloy takes place at much favorable conditions (i.e., at higher temperature and at longer oxidation times) than in case of E110, and the E110G cladding picks up much less hydrogen during oxidation in steam than the E110 alloy.

ACKNOWLEDGMENTS

The performed test series was supported by the Paks Nuclear Power Plant, Hungary. The writers are grateful to Alajos Ö. Kovács (Material Physics Department, University, Budapest) for the TMA and DSC measurements.

References

[1] Gerasimov, V. V., and Monakhov, A. S., 1982, *Materials for Nuclear Technology*, Energoatomizdat, Moscow (in Russian).

[2] IAEA, "Design and Performance of WWER Fuel," *Technical Report Series No. 379*, International Atomic Energy Agency, Vienna, 1996.

[3] Shebaldov, P. V., Peregud, M. M., Nikulina, A. V., Bibilashvili, Y. K., Lositski A. F., Kuz'menko, N. V., Belov, V. I., and Novoselov, A. Y., "E110 Alloy Cladding Tube Properties and Their Interrelation With Alloy Structure-Phase Condition and Impurity Content," *Proceedings of the 12th International Symposium on Zirconium in the Nuclear Industry*, Toronto, ON, ASTM STP 1354, ASTM International, West Conshohocken, PA, 2000, pp. 545–558.

[4] Smirnov, A. V., Markov, D. V., Smirnov, V. P., Polenok, V. S., Ivashchenko, A. A., and Strozhuk, A. V., "Results of Post-Irradiation Examination of VVER Fuel Assembly Structural Components Made of E110 and E635 Alloys," *Proceedings of the 6th International Conference on WWER Fuel Performance, Modelling and Experimental Support*, Albena, Bulgaria, Sept 19–23, 2005, pp. 231–243.

[5] Novikov, V. V., Markelov, V. A., Shishov, V. N., Tselishchev, A. V., and Balashov, A. A., "Results of Post-Irradiation Examinations (PIE) of E110 Claddings and Alloy Upgrading for VVER," *Transactions of TOPFUEL* 2006, Poster Session II, http://www.euronuclear.org/events/topfuel/transactions/Topfuel-Poster%20Session%20II.pdf

[6] Smirnov, V. P., Markov, D. V., Smirnov, A. V., Polenok, V. S., Perepelkin, S. O., and Ivashchenko, A. A., "VVER Fuel: Results of Post Irradiation Examination," *Proceedings of the 2005 Water Reactor Fuel Performance Conference*, Kyoto, Japan, Oct 2–6, 2005, pp. 217–226.

[7] Yegorova, L., Lioutov, K., Jouravkova, N., Konobeev, A., Smirnov, V., Chesanov, V., and Goryachev, A., "Experimental Study of Embrittlement of Zr-1 %Nb VVER Cladding Under LOCA-Relevant Conditions," *NUREG/IA-0211*, 2005, http://pbadupws.nrc.gov/docs/ML0511/ML051100343.pdf

[8] Hózer, Z., Győri, C., Matus, L., and Horváth, M., "Ductile-to-Brittle Transition of Oxidised Zircaloy-4 and E110 Claddings," *J. Nucl. Mater.*, Vol. 373, 2008, pp. 415–423.

[9] Yan, Y., Burtseva, T. A., and Billone, M. C., "High-Temperature Steam-Oxidation Behavior of Zr-1Nb Cladding Alloy E110," *J. Nucl. Mater.*, Vol. 393, 2009, pp. 433–448.

[10] Steinbrück, M., Birchley, J., Boldyrev, A. V., Goryachev, A. V., Grosse, M., Haste, T. J., Hózer, Z., Kisselev, A. E., Nalivaev, V. I., Semishkin, V. P., Sepold, L., Stuckert, J., Vér, N., and Veshchunov, M. S., "High-Temperature Oxidation and Quench Behaviour of Zircaloy-4 and E110 Cladding Alloys," *Prog. Nucl. Energy*, Vol. 52, 2010, pp. 19–36.

[11] Perez-Feró, E., Győri, C., Matus, L., Vasáros, L., Hózer, Z., Windberg, P., Maróti, L., Horváth, M., Nagy, I., Pintér-Csordás, A., and Novotny, T., "Experimental Database of E110 Claddings Exposed to Accident Conditions," *J. Nucl. Mater.*, Vol. 397, 2010, pp. 48–54.

[12] Nikulin, S. A., Rozhnov, A. B., Belov, V. A., Li, E. V., and Glazkina, V. S., "Influence of Chemical Composition of Zirconium Alloy E110 on Embrittlement Under LOCA Conditions—Part 1: Oxidation Kinetics and Macrocharacteristics of Structure and Fracture," *J. Nucl. Mater.*, Vol. 418, 2011, pp. 1–7.

[13] Hózer, Z., Győri, C., Horváth, M., Nagy, I., Maróti, L., Matus, L., Windberg, P., and Frecska, J., "Ballooning Experiments With VVER Cladding," *Nucl. Technol.*, Vol. 152, 2005, pp. 273–285.

[14] Chung, H., "The Effects of Aliovalent Elements on Nodular Oxidation of Zr-Base Alloys," Proceedings of the 2003 Nuclear Safety Research Conference, Oct 20–22, 2003, NUREG/CP-0185, pp. 283–298.

[15] Yegorova, L., Lioutov, K., Smirnov, V., Goryachev, A., and Chesanov, V., "LOCA Behavior of E110 Alloy," Proceedings of the 2003 Nuclear Safety Research Conference, Oct 20–22, 2003, NUREG/CP-0185, pp. 123–140.

DISCUSSION

Question from Robert J. Comstock, Westinghouse Electric Co.:—What is the current understanding regarding why sponge-based E110G shows a dramatic improvement in breakaway oxidation performance?

Authors' Response:—There are two reasons mentioned in the literature to explain the potential reasons for breakaway oxidation:

a) The presence of some impurities (e.g. halogens) can be deleterious, and can lead to increased susceptibility to nodular oxidation.

b) Experiments with polished E110 samples showed that surface treatment can be used to avoid breakaway oxidation.

In the present study the two cladding tubes had the same surface roughness, but the content of impurities was different. Probably the higher content of halogens in the E110 could cause the observed breakaway phenomena.

Question from K. Kapoor, NFC:—Please provide individual concentrations of Si, C, Ni, Cl, N, F, etc., for the two alloys?

Authors' Response:—The F content was 30 ppm in E110 and 10 ppm in E110G, while the Cl content was 3 ppm in E110 and 1 ppm in E110G. The concentration of other above listed elements has not been identified yet.

Question from Mirco Grosse, Karlsruhe Inst. Of Technology:—The improvement of the oxidation and hydrogen uptake is impressive. What is the time scale for licensing and application of this material?

Authors' Response:—The new alloy has already been tested in Russia in VVER-440 reactors. The change in the composition of the alloy does not need necessarily new licensing procedures. Taking into account that the behavior of the new alloy is very similar to the currently used one in normal operational conditions, and its parameters are much better for accident situations, the new alloy can be quickly introduced in the countries where the E110 is used.

Question from Martin Steinbrück, Karlsruhe Inst. Of Technology:—Did you compare your results on E110G to M5?

Authors' Response:—The E110G and M5 alloys have not been directly compared in the present test series. The comparison with M5 oxidation data published by AREVA shows that E110G and M5 oxidation kinetics at high temperature were very close to each other. The direct comparison would be desirable in the future to

compare the behavior of two Nb containing Zr alloys produced in different factories with very similar compositions. Our research center could carry out such comparative tests if M5 alloy was accessible to us.

Question from Ron Adamson, Zircology Plus:—Were the surface conditioning processes the same for both alloys? For instance, was one belt polished and the other etched, etc.?

Authors' Response:—According to the Russian fuel supplier the surface conditioning processes was the same for both alloys.

Questions from S. Anantharaman, BARC Mumbai Q1:—What is the reason for choosing ring compression tests instead of ring tension test?

Authors' Response:—Both ring compression and ring tension tests can be used to determine the ductile-to-brittle transition of oxidized cladding, since the load-displacement curves from both tests show the characteristic behavior of ductile or brittle material. The ring compression tests can be carried out with regular ring shaped tube samples. For tension testing additional manufacturing may be needed to produce a reduced section in the ring. Our laboratory traditionally applies ring compression tests, and in order to compare the new results with the data of previous studies we continue to use this technique.

Q2:—What should be the limiting value of the hydrogen content of the fuel cladding in your view?

Authors' Response:—According to our measured data the Zr cladding shows brittle behavior above 500 ppm H content.

Q3:—What is the effect of cladding hydrogen content on the % ECR?

Authors' Response:—Our experiments with H pre-charged Zr cladding tubes showed that H content up to 600 ppm does not change the oxidation kinetics in high temperature steam. However, the mechanical testing of oxidized Zr tubes indicated that the H pre-charged samples became brittle at lower ECRs, compared to as received cladding.

Questions from P. Barberis, CEZUS Research Center:—E110G contains much lower Hf than E110. Does it mean that the Zr-Hf separation process was changed when going to Zr sponge?

Authors' Response:—It was the intention of the fuel supplier to reduce the Hf content of the alloy, and obviously they had some changes in the separation process.